International Journal of Nanomedicine

Dovepress
open access to scientific and medical research

Open Access Full Text Article

ORIGINAL RESEARCH

Antioxidant Carbon Dots Nanozyme Loaded in Thermosensitive in situ Hydrogel System for Efficient Dry Eye Disease Treatment

Wei Wei[1,2,*], Haili Cao[2,*], Di Shen[2], Xiyu Sun[2], Zhenzhen Jia[1], Mingzhen Zhang[1]

[1]School of Basic Medical Sciences, Xi'an Jiaotong University Health Science Center, Xi'an, Shaanxi, 710061, People's Republic of China; [2]Xi'an No.1 Hospital, Shaanxi Institute of Ophthalmology, Shaanxi Key Laboratory of Ophthalmology, Clinical Research Center for Ophthalmology Diseases of Shaanxi Province, First Affiliated Hospital of Northwestern University, Xi'an, Shaanxi, 710002, People's Republic of China

*These authors contributed equally to this work

Correspondence: Zhenzhen Jia; Mingzhen Zhang, Email jzz324716@stu.xjtu.edu.cn; mzhang21@xjtu.edu.cn

Purpose: Dry eye disease (DED) is a multifactorial ocular surface disease with a rising incidence. Therefore, it is urgent to construct a reliable and efficient drug delivery system for DED treatment.

Methods: In this work, we loaded C-dots nanozyme into a thermosensitive in situ gel to create C-dots@Gel, presenting a promising composite ocular drug delivery system to manage DED.

Results: This composite ocular drug delivery system (C-dots@Gel) demonstrated the ability to enhance adherence to the corneal surface and extend the ocular surface retention time, thereby enhancing bioavailability. Furthermore, no discernible ocular surface irritation or systemic toxicity was observed. In the DED mouse model induced by benzalkonium chloride (BAC), it was verified that C-dots@Gel effectively mitigated DED by stabilizing the tear film, prolonging tear secretion, repairing corneal surface damage, and augmenting the population of conjunctival goblet cells.

Conclusion: Compared to conventional dosage forms (C-dots), the C-dots@Gel could prolong exhibited enhanced retention time on the ocular surface and increased bioavailability, resulting in a satisfactory therapeutic outcome for DED.

Keywords: dry eye disease, carbon dots nanozyme, thermosensitive in situ gel, composite ocular drug delivery system

Introduction

Dry eye disease (DED), also known as dry keratoconjunctivitis, is a prevalent multifactorial ocular surface disease that has impacted the daily functioning of millions of people around the world.[1] DED is characterized by a reduced volume of tears, abnormal corneal epithelial cells, and loss of conjunctival goblet cells,[2] resulting in compromised vision and quality of life.[3] Recent studies indicate a growing prevalence of DED worldwide, attributed to shifts in modern lifestyles, the popularity of corneal contact lenses, and environmental pollution.[4–6]

As a kind of multifactorial inflammatory disease, the pathogenesis of DED remains poorly understood. Researchers have found that the reactive oxygen species (ROS) are linked to DED and are believed to contribute to its pathological development.[7–9] Therefore, targeting the overproduced reactive oxygen species (ROS) might be beneficial in efficiently managing inflammation in DED.[8,10] Under normal circumstances, the antioxidant system, consisting of endogenous antioxidant enzymes such as superoxide dismutase (SOD) and small molecules plays a crucial role in maintaining redox homeostasis. While the overproduction of ROS and reduced activity of anti-oxidase SOD have an unbalance in DED. Therefore, some eye drops with antioxidants, such as vitamin A, quercetin, and selenoprotein P, were reported to be effective in protecting the ocular surface from oxidative stress.[10]

However, these treatments often yield unsatisfying results and have a high recurrence rate. At present, the major challenge in the drug-based treatment of DED is the limited residence time of conventional eye drops in the eye due to its

Received: 25 December 2023
Accepted: 30 April 2024
Published: 7 May 2024

unique structure, resulting in low bioavailability (< 5%).[11] High doses and frequent administration are required to achieve the expected outcome which brings increased side effects and poor patient compliance.[12] Therefore, it is crucial to explore novel and efficient DED therapies to minimize the frequency of administration, thereby improving ocular bioavailability and enhancing patient compliance.[13] To address the challenge, researchers have built diverse drug delivery systems, including polymer micelles, hydrogels, and metal frame materials, to improve the retention time and increase the permeability of drugs.[14–16]

To update, various hydrogel dosages have been developed based on synthetic polymers or peptides.[17–21] Among them, in-situ gelling based on environmentally sensitive polymers would undergo structural changes in response to variations in specific conditions such as pH, temperature, and ionic strength.[10,20] In the context of ophthalmic applications, in-situ forming gels transition from a liquid state upon instillation into the eye to rapidly form viscoelastic gels within the cul-de-sac, adapting to environmental cues. This controlled gelation process enables sustained drug release under physiological conditions.[22] Consequently, the duration of the gel formed in situ is prolonged, and the drug is released in a sustained manner which leads to enhanced bioavailability, minimized systemic absorption, and reduced frequent dosing regimen resulting in improved patient compliance.[23,24]

Nanozyme, artificial enzyme with catalytic activity comparable to natural enzyme, offer advantages including small size (particle size only 3~5 nm),[25] stability in harsh conditions, good water solubility, strong photostability, good biocompatibility, ease of mass synthesis, and low-cost modification.[26] These nanozymes exhibit enzymatic reaction kinetics and belong to a novel class of mimetic enzymes. The distinctive properties of C-dots nanozyme have led to their utilization in various medical applications, including biosensing, drug delivery, and biological imaging.[27] There have been a few reports on the application of nanozyme in the eyes.[28–31] The small particle size of nanozyme enhances their ability to penetrate tissues, thereby improving drug permeability in ocular settings.[32] It has been reported that many carbon nanomaterials can act as electron donors or acceptors, endowing them as pro-oxidants or antioxidants.[33] Furthermore, the advantages of inherent biocompatibility and low cost make carbon-based nanomaterials have potential application for DED treatment. In our previous study, we synthesized the Carbon dots (C-dots) based on activated charcoal, which was demonstrated to have very high SOD-like activity. Therefore, it has the potential to safeguard the DED against inflammatory response caused by ROS.

This study presents the development of a C-dots nanozyme thermosensitive in situ gel system (C-dots@Gel) for controlled drug release. The system was created by incorporating C-dots nanozyme into temperature-sensitive hydrogel using a swelling loading technique (Scheme 1). Various parameters including appearance, pH value, gelation temperature, gelation temperature after mixing with artificial tears, gelation time, gelation ability, in vivo gelation validation, retention time on the ocular surface of mice, stimulating effect on the ocular surface of mice, and in vivo biosafety were studied. The results of tear secretion, tear film break-up time (TBUT), corneal fluorescein staining, and histology of cornea and conjunctiva were used to evaluate the therapeutic effect of C-dots@Gel on DED.

Materials and Methods

Materials

Benzalkonium chloride (12,060) was supplied by Sigma Aldrich (Shanghai, China). Hydroxypropyl methylcellulose (HPMC E50, H811095) was purchased from Macklin Biochemical Technology (Shanghai, China). Poloxamer 407 (S7071) and 188 (S7070) were supplied by Solabao Life Sciences (Beijing, China). Carbon dots (C-dots) nanozyme was synthesized in our laboratory. Tear Test Strips were supplied by Tianjin Jingming New Technology Development. (Beijing, China). Sodium fluorescein (AR) was supplied by Maikun Chemical (Shanghai, China). All aqueous solutions used in this work were prepared with deionized water with a resistivity of 18.2 MΩ·cm.

Synthesis of the C-Dots

C-dots were synthesized according to our previous study. Firstly, 0.5 g of activated carbon was added to a boiling solution composed of 50 mL of mixed acid (V_{HNO3}:V_{H2SO4} =1:1). After reacting for 1.5 h at its boiling point, the obtained solution was cooled to room temperature. The aforementioned samples were then subjected to neutralization via

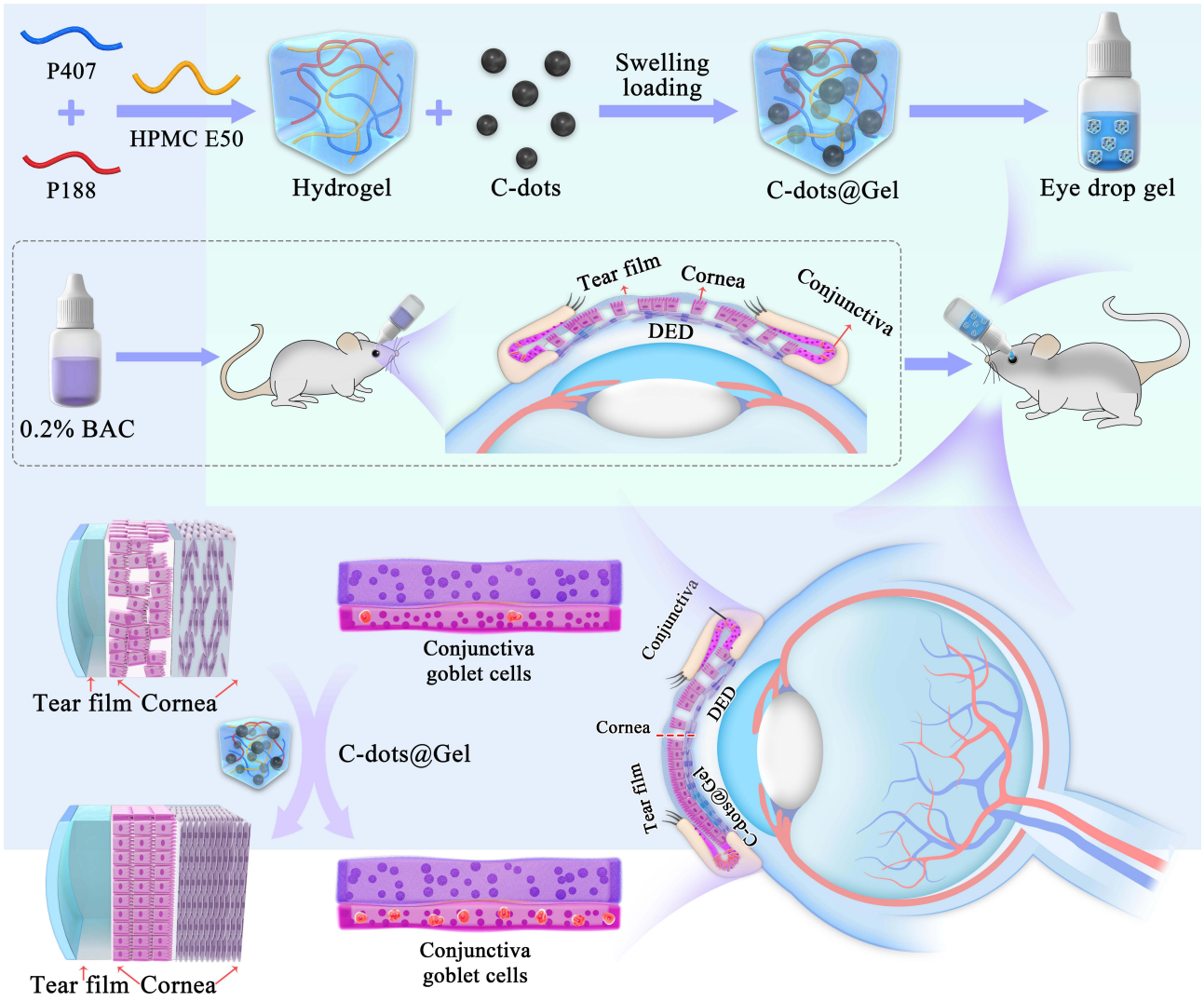

Scheme 1 Schematic diagram of the C-dots@Gel preparation and its effect on dry eye disease (DED).

the addition of $NaHCO_3$ and then filtered through a 0.22 μm aqueous membrane. After a week-long dialysis process with water changes occurring 4–5 times per day, the dialyzed solution was subsequently filtered again through a 0.22 μm aqueous membrane to eliminate any remaining insoluble material. Subsequently, the filtrate liquid was subject to ultrafiltration via ultrafiltration tubes with a molecular retention capacity of 100 kDa. After separation, the obtained C-dots were acquired and subsequently lyophilized for further use.

Preparation of Blank Thermosensitive in situ Gel

Poloxamer 407, 188, and HEMC E50 were gradually introduced into the water at 4°C and thoroughly mixed using a glass rod. Subsequently, the mixture was subjected to magnetic stirring for 1 h and then refrigerated at 4°C overnight.

Evaluation of Blank Thermosensitive in situ Gel

To determine the gelation temperature T1 (phase change temperature), 2 mL of hydrogel solution was placed in a covered test tube in a water bath (20°C). The temperature was monitored using a precision thermometer (accuracy of 0.1°C), And when it increased by 0.1°C (equilibrium at each temperature point for 5min), the test tube was removed and quickly tilted to 45° to observe gelling. The solution was considered a hydrogel when no flow was observed for 30s, indicating the phase transition temperature T1.[34]

When the human eye blinks, there is approximately 7 μL of tear fluid in the conjunctival sac. The average volume of a single drop of commercially available eye drops ranges from 25 μL to 56 μL, with an average of 40 μL. Usually, when hydrogel solution enters the conjunctival sac, two conditions may occur the hydrogel solution may either undergo gelation without dilution by tears, thereby optimizing ocular retention time, or it may first mix with tears before forming a gel. The situation after ocular administration must be somewhere in between. The gelation temperature (T2) was determined by combining a temperature-sensitive in situ hydrogel with simulated tears at a ratio of 40:7.[35] To confirm the T2, 2 mL of the hydrogel solution was placed in a 5 mL capped test tube and immersed in a water bath at 40°C. The gelation process was monitored by tilting the tube to a 90° angle and the time at which no solution flow was observed as the gelation time. To assess gelation capacity, 200 μL of hydrogel solution was added to a test tube containing 2 mL of simulated tear fluid (STF) with a pH of 7.4, and the temperature was stabilized at 37±2°C. The process of hydrogel formation was visually observed, noting the time of hydrogel formation and dissolution.[36] Gelation ability was evaluated as follows: (-) indicating no gelation; (+) indicating gelation within a few minutes and rapid dispersion; (++) indicating immediate gelation with retention for several hours.

Formulation Design of Blank Thermosensitive in situ Gel

It has been shown that when the concentration of Poloxamer is higher than 15% (w/v), it is in a liquid state at room temperature and could form a colorless transparent hydrogel on the ocular surface. 3^2 randomized full factorial design was chosen to study the effects of Poloxamer 407 and 188 concentrations on thermosensitive in situ gels. In this design, the proportions of Poloxamer 407 (A, 20%, 21%, 22%) and Poloxamer 188 (B, 0.75%, 1.00%, 1.25%) were used as independent variables; the gelation temperatures T1 (Y1), T2 (Y2) and gelation time (Y3) were used as dependent variables.

Preparation and Evaluation of C-dots@Gel

The C-dots nanozyme solution (dissolved in purified water) was loaded into the preferred thermosensitive in situ gel by swelling loading method to construct C-dots@Gel. It was dissolved for 6–8 hours at 4°C to achieve an equilibrium swollen state. It was also evaluated by its appearance, pH value, gelation time, gelation temperature, and gelation capacity.

Validation of in vivo Gelation

In Balb/c mice, 5 μL of blank in situ gel or C-dots@Gel (20 μg/mL, 40 μg/mL) were dropped into the conjunctival sac, and observing the changes of the gel solution on the ocular surface.

Precorneal Retention Time

To study the precorneal retention of C-dots@Gel, sodium fluorescein was dissolved in C-dots or C-dots@Gel to obtain sodium fluorescein-labeled C-dots or C-dots@Gel. Then 2 μL of the sodium fluorescein-labeled C-dots or C-dots@Gel was topically dropped into the subconjunctival sac of the eye.[37] The green fluorescence on the ocular surface was observed under blue light with a slit lamp at specific time intervals.

Ocular Surface Irritation Test and Biocompatibility in vivo

To evaluate the biocompatibility of C-dots@Gel in vivo, experimental mice were randomly divided into three groups: (1) control group; (2) C-dots group; (3) C-dots@Gel group (3 mice in each group). Briefly, 5μL of PBS, C-dots, or C-dots@Gel were dropped into the conjunctival sacs of both eyes of the mice twice a day on time (10 a.m. and 5 p.m.) for 7 consecutive days. Corneal fluorescein staining, corneal edema, corneal neovasculature, and corneal and conjunctival inflammation were evaluated by slit-lamp examination on day 0 and day 7. Finally, the mice were executed, and the eyeballs were collected for hematoxylin and eosin (HE) staining. To test the biocompatibility of C-dots@Gel, the heart, liver, spleen, lung, and kidney tissues of each group were stained by H&E, and observed by optical microscope, and the blood routine examination was performed.

Mice DED Model

Female C57BL/6 mice (6–8 w, 18–20 g) were purchased from Beijing Vitonglihua Experimental Animal Technology (SCXK (Jing) 2021–0006). All experimental protocols involving animals were performed in accordance with the Guidelines for Care and Use of Laboratory Animals of Xi'an Jiaotong University and approved by the Animal Ethics Committee of Xi'an Jiaotong University.

The male C57BL/6 mice aged 6 to 8 weeks were fed in air ventilation conditions for one week. Inclusion criteria: healthy mice without corneal ulcers and old white spots. To establish the DED model, 5 μL of 0.2% BAC solution was dropped into the conjunctival sac of both eyes twice a day (10 a.m. and 5 p.m.) for 14 consecutive days.[38] On days 0, 3, 7, 10, and 14, tear volume, TBUT, corneal fluorescence staining score, and body weight were recorded. All tests were repeated three times.

In vivo Evaluation of Therapeutic Efficiency of C-dots@Gel in DED

The DED model mice and healthy C57BL/6 mice were divided into four groups: (1) control group, (2) DED group, (3) C-dots group, and (4) C-dots@Gel group. Each group received topical administration of 5μL of PBS, PBS, C-dots, or C-dots@Gel to both eyes twice daily (10 a.m. and 5 p.m.) for 7 consecutive days. Tear volume, TBUT, corneal fluorescence staining score, and body weight were recorded on day 1, day 4, and day 7 post-treatment. To measure tear volume, a 1.5 mm×30 mm strip of tear filter paper was inserted into the outer 1/3 of the conjunctival sac of the lower lid of mice for 4 min, and the wetted length of the paper indicated the tear volume.[39] TBUT was assessed under a slit lamp microscope equipped with cobalt blue light after 1μL of 1% fluorescein sodium solution was dropped into the conjunctival sac of mice until the first dry spot appeared after the last blink.[40] Fluorescein sodium staining score combined with the TBUT test to evaluate corneal epithelial injury. The cornea was divided into 5 regions and scored based on the level of staining: 0 for no staining, 1 for slight spot staining (< 30 spots), 2 for exceeding 30 punctate staining spots without diffuse staining, 3 for severe diffuse staining without positive plaque, 4 for severe plaque/plaque staining. The final score was obtained by adding the scores of the five regions. To evaluate histological variation, the eyeballs of the mice were collected for HE staining, and the cornea and conjunctiva were pathologically analyzed under the optical microscope.

Statistical Analysis

The data were expressed as mean ± standard deviation (S.D.). Statistical analysis was performed using GraphPad Prism 8.0. One-way analysis of variance (ANOVA) was performed to analyze the differences between groups, and $P < 0.05$ was considered statistically significant.

Results and Discussion

Characterization of C-Dots

To explore the ROS scavenging capabilities of the C-dots, the SOD-like activity of the C-dots was assessed using the nitro blue tetrazolium (NBT) method. NBT, serving as a probe for superoxide O_2^-, was reduced to blue formazan, with peak absorption at 560 nm. The SOD enzyme acts to scavenge $\bullet O_2^-$, thereby preventing the formation of formazan. Analysis of the kinetic curves at 560 nm revealed a positive correlation between the SOD-like activity of the C-dots and their concentrations (Figure 1A). Furthermore, the SOD-like activity of the C-dots was assessed using a total SOD activity detection kit that utilizes WST as a basis. The enzymatic activity of the C-dots was calculated to be about 4612.72 U/mg based on the WST results (Figure 1B).

To assess the antioxidant potential of the C-dots, their overall antioxidant capacity was evaluated using a Total Antioxidant Capacity Assay Kit. In this method, the compound 2.2'-azino-bis (3-ethyl-benzthiazoline-6-sulfonic acid) (ABTS) serves as a chromogenic reagent that undergoes oxidation to form green ABTS+ in the presence of oxidizing agents. The presence of antioxidants inhibits the formation of ABTS+, allowing for the determination of antioxidant capacity through the measurement of ABTS+ absorption at 734 nm. The inhibition rate of ABTS+ increased with higher

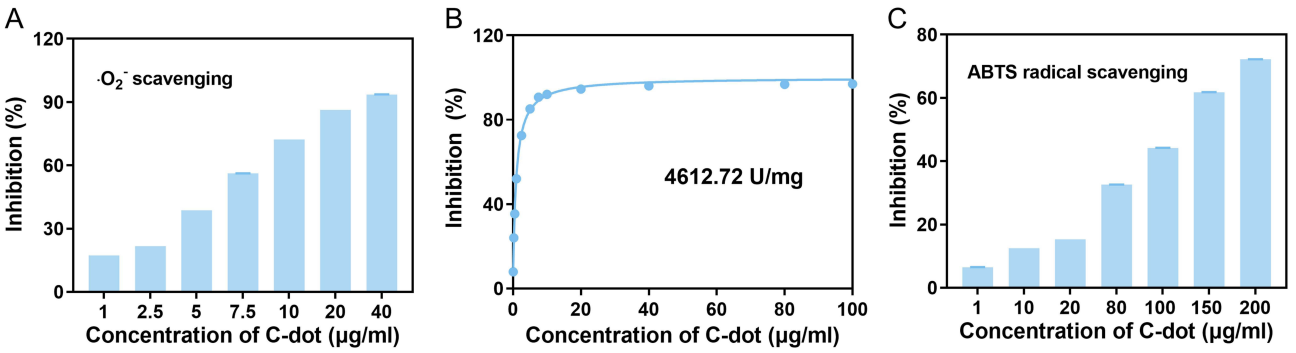

Figure 1 The properties of the C-dots. (**A**) The capacity of C-dots to eliminate $\cdot O_2^-$. (**B**) The SOD-like activity in the C-dots of different concentrations. (**C**) The ABTS radical scavenging ability of the C-dots.

concentrations of C-dots, reaching above 60% at a concentration of 150 μg/mL, indicating the ability of C-dots to scavenge reactive oxygen species (Figure 1C).

Formulation Design of Blank Thermosensitive in situ Gel

Initially, hydrogel formulations with different ratios of P407 and P188 were designed (Table S1).[27,41] The desired T1 temperature ranged from 25°C to 34°C, and T2 was guaranteed to be around 34°C (the ocular surface temperature of a normal person).[42,43] Then, F10-15 was found to meet the requirements. It is important to note that significant variability in measured data for gelation time and capacity was observed due to differences in initial sample temperature. To mitigate this, all samples were standardized to an initial temperature of 25°C during testing.

With the ratio of P407 (A, 20%, 21%, 22%) and P188 (B, 0.75%, 1.00%, 1.25%) as independent variables, the model fitting was carried out to select the most desirable proportional formulation. The parameters under the above ratios were measured. The gelation temperature T1 (Y1), T2 (Y2) and gelation time (Y3) were 23.40±0.10~29.10±0.06°C, 32.63±0.15~40°C, 2.01 ±0.03~9.28±0.27 s, respectively (Table S1). The results were processed by Design-expert v 8.0.6 to obtain the multiple linear equations and binary multiple equations of gelation temperature T1, T2, and gelation time. The coefficients of the equations were analyzed by variance. Combined with the correlation of multivariate linear equation and quadratic polynomial equation, in principle, the model with good correlation should be selected, so Y1 and Y3 chose the quadratic multinomial model, Y2 chose the multivariate linear model, and the results are as follows:

$Y1= -200.3+24.81667*A-16.73333*B+0.20*A*B-0.65*A^2+4.80*$ ($P=0.0051$, $R^2=0.9868$)

$Y2= 119.01111–3.90*A-1.27333*B$ ($P=0.0005$, $R^2=0.9185$)

$Y3=768.00111–65.34667*A-106.58667*B+4.52*A*B+1.39333*A^2+4.21333*B^2$ ($P=0.0366$, $R^2=0.9525$) The models were significant at $P < 0.05$.

According to the fitting equations, a design expert was used to draw the three-dimensional effect surface and contour maps of independent variables A and B to Y1, Y2, and Y3, respectively. The proportions of P407 and P188 have a significant effect on the gelation temperature T1, T2, and gelation time, and all the effects were negative. The concentration of P407 had more influence on the T1, T2, and gelation time (the more curved the curve is, the greater the effect of this factor). As the P407 concentration increases, the gelation temperatures T1 and T2 decrease. The formulated system with a high concentration of Poloxamer leads to hydrogel formation even below normal room temperature. These factors were taken into consideration when selecting an optimized batch. The contour map is the projection of the 3D effect map at the bottom, and the influence trend is the same as that of the 3D effect map (Figure 2).

Therefore, to maintain the desired liquid of the hydrogel solution at room temperature (25°C) and promote gel formation on the animal eye surface (34°C), F11 (P407=21%, P188=1.0%) was selected as the optimal formation. It is reported that high concentrations of P407 may lead to ocular surface irritation. To mitigate this potential issue while maintaining the gelation property, a low-viscosity viscosity enhancer HPMC E50 was added into the formula. The dosage of HPMC E50 was determined based on the dosage of P188, which had little influence on the dependent variable. In addition, the gelation capacity is a critical factor considered in the selection of the optimal formula (Table S1 and Figure 3A). The final composition of the hydrogel formula

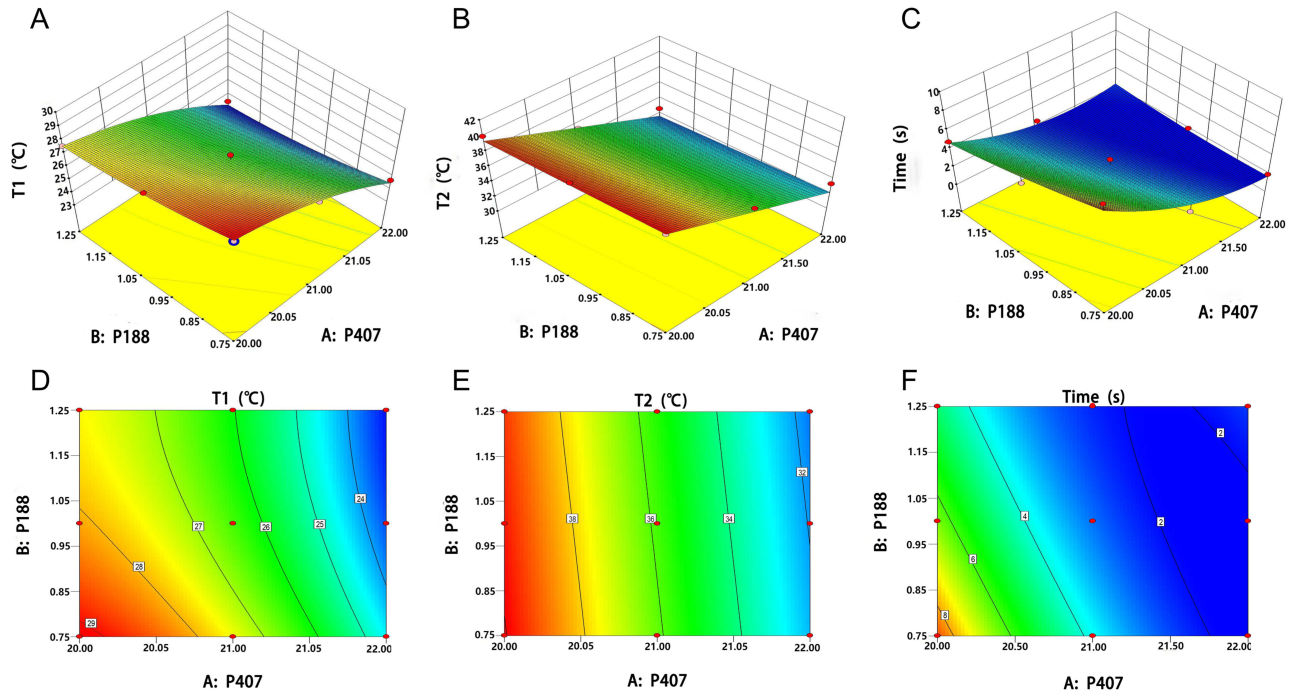

Figure 2 Three-dimensional 3D response surface and contour plot showing the effect of T1, T2, and gelation time. (**A**) Y1 (Gelation temperature T1), and (**B**) Y2 (Gelation temperature T2) before and after simulated tear dilution. (**C**) Y3 (Gelation time). (**D**–**F**) The contour map is 3D with a projection at the bottom, corresponding to (**A**–**C**).

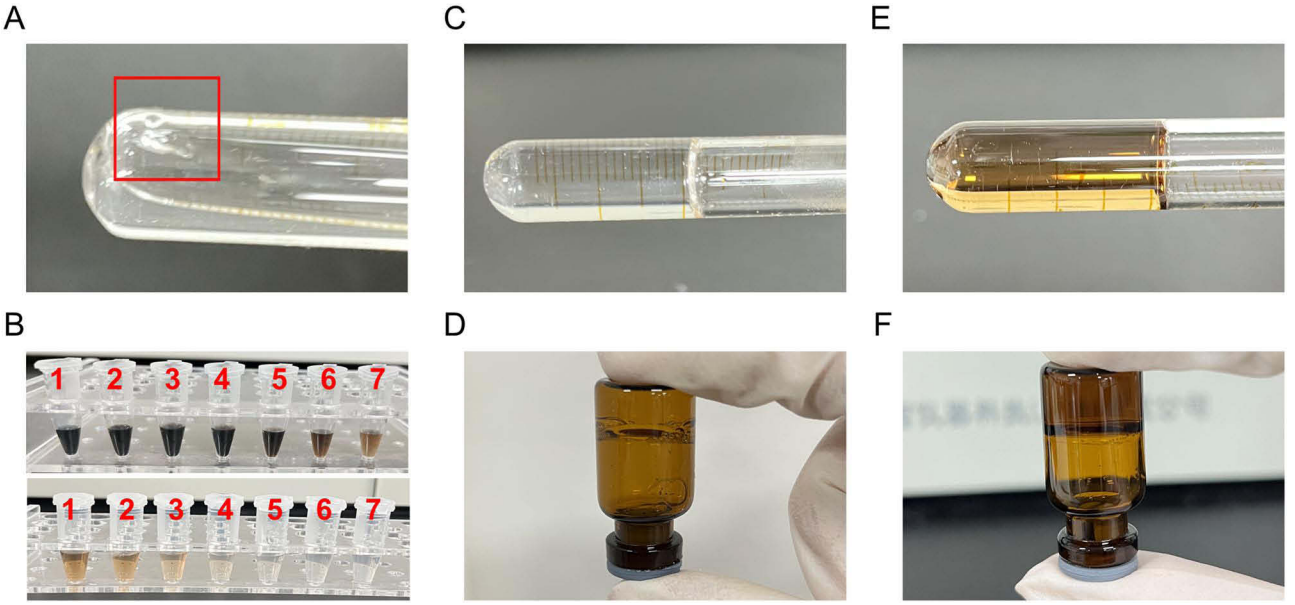

Figure 3 Appearance of gels. (**A**) Gelation capacity. (**B**) The appearance of different concentrations of C-dots loading into blank in situ gel (1 to 7 represents the concentration of 100, 80, 40, 20, 10, 5, and 2.5 μg/mL, respectively). (**C** and **D**) Blank gel and (**E** and **F**) C-dots@gel at gelation temperature.

consisted of P407=21%, P188=1.0%, and HPMC E50=1.0%. The gelation temperature was determined to be T1=26.67°C and T2=34.00°C. The gelling process can be completed within approximately 3 s (at 40°C), and the gelation ability is good (at 37°C, hydrogel and tear mixture, ++).

Preparation of C-dots@Gel

To explore the impact of C-dots nanozyme on the blank in situ gel, various volumes of C-dots nanozyme aqueous solutions (0.2 mL, 0.1 mL, 0.05 mL, 0.02 mL) were mixed with 10 mL of the blank in situ hydrogel solution. A notable impact on T2 of C-dots@Gel was observed with the addition of 0.2 mL of C-dots, while varying volumes of 0.1 mL, 0.05 mL, and 0.02 mL showed minimal differences in T2. To ensure the accuracy of sampling, the volume ratio of C-dots solution and in situ hydrogel was determined to be 1:100 (Table S2 and Figure 3B).

Evaluation of C-dots@Gel

The blank in situ gel was colorless, clear, and transparent (Figure 3C and D), while the C-dots@Gel appeared yellowish, clear, uniformly dispersed, and transitioned into a semi-solid solution at the gelation temperature T1 (Figure 3E and F). The pH of various concentrations of C-dots@Gel was approximately 6.50 (Table S2), Falling within the acceptable pH range for ophthalmic preparations (3.5–8.5). This pH range is considered safe for patients, as it does not have a significant sensitizing effect on patients.[44]

The T1 data for various concentrations of C-dots@Gel are around 36°C (Table S2), a temperature comparable to that T1 of the blank in situ gel, indicating that the C-dots concentration has minimal influence on gelation temperature T1 of C-dots@Gel. The T2 data for C-dots@Gel at concentrations of 2.5 and 5 μg/mL both measured around 34°C, mirroring the T2 of the blank in situ gel, indicating that low concentrations of C-dots nanozyme did not significantly alter the T2 of C-dots@Gel. The T2 of C-dots@Gel at concentrations ranging from 10 to 40 μg/mL were found to be within the range of 35.83–36.10°C, which was 1~2°C higher than that of blank in situ gel. Conversely, C-dots@Gel at concentrations of 80 and 100 μg/mL did not fully gel at the upper limit of 40°C. These results indicated that the higher concentration of C-dots nanozyme has a notable impact on T2 of the C-dots@Gel. The gelation properties of different concentrations of C-dots@Gel had minimal deviation when compared to the blank in situ gel, indicating that the different concentrations of C-dots nanozyme had little effect on the gelation ability of C-dots@Gel (Table S2).

Validation of in vivo Gelation

It was found that at concentrations of C-dots@Gel of 20 and 40 μg/mL, the C-dots@Gel diluted with artificial tears underwent gelation at approximately 36°C (T2≈36°C). However, the literature showed that the average ocular surface temperature of a normal human individual is 33.7°C, suggesting that T2 should be closer to 34°C.

When 5 μL of blank in situ gel and C-dots@Gel (20 μg/mL, 40 μg/mL) were respectively dropped into the conjunctival sac of Balb/c mice, gelation occurred within a rapid timeframe of approximately 3 to 4 seconds (Figure 4). The T2 of 20 and 40 μg/mL of C-dots@Gel was 36°C, exceeding the surface temperature of the eye. However, both concentrations rapidly formed a hydrogel quickly in the mouse eye. This discrepancy may be attributed to the inability to fully replicate the conditions of the drug on the mouse ocular surface in vitro, leading to a discrepancy between the T2 data obtained and the actual temperature of the mouse ocular surface (34°C).

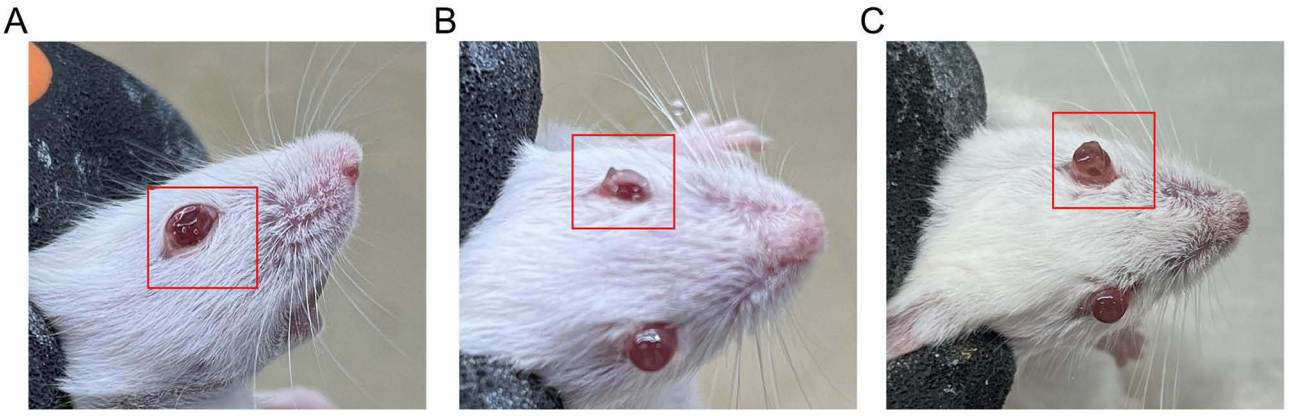

Figure 4 The pictures of gelling on the ocular surface. (**A**) blank Gel. (**B** and **C**) C-dots@Gel (20 μg/mL and 40 μg/mL).

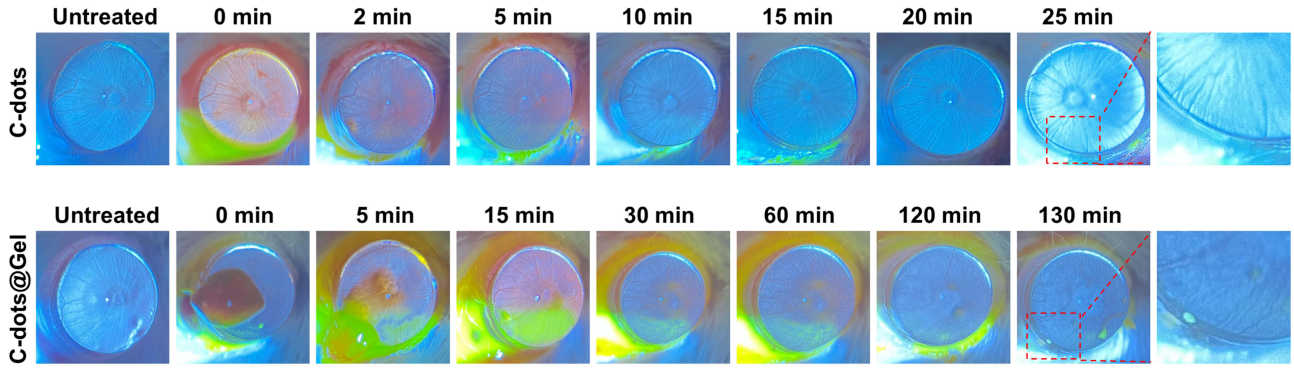

Figure 5 Precorneal Retention Time evaluation. Precorneal retention of sodium fluorescein that loaded C-dots and C-dots @ Gel after topical instillation in mice eye.

Precorneal Retention Time

After the administration of fluorescein sodium-labeled C-dots aqueous solution into the conjunctival sac of mice for 20 min, it was completely cleared from the ocular surface (Figure 5). Conversely, fluorescein sodium-labeled C-dots@Gel rapidly formed a hydrogel upon instillation into the eye. This hydrogel was observed to dissolve or be expelled by tears to the orbit at approximately 15 min (and the outside of the eye). It could be maintained on the ocular surface for about 120 minutes and almost eliminated from the ocular surface at 130 minutes. Compared with C-dots aqueous solution, C-dots@Gel significantly extended the retention time of the C-dots in front of the cornea (Figure 5).

Ocular Surface Irritation Test and Biocompatibility in vivo

Ocular surface irritation and in vivo toxicity are important aspects to be considered in the study of new ophthalmic formulations. After administration of C-dots@Gel and C-dots into the ocular surface for 7 days, the irritation and in vivo toxicity were evaluated.

Compared with the pre-administration group, mice that received drug administration exhibited a smooth ocular surface without corneal edema, corneal neovascularization. Additionally, there was no significant sodium fluorescein staining under cobalt blue light (Figure 6A). These results indicated that C-dots and C-dots@Gel hardly have a stimulating effect on the ocular surface. The structure and integrity of the cornea, conjunctiva, iris, and retina were further assessed by H&E staining. In comparison to the control group, the corneal surface epithelial cells of mice in the C-dots and C-dots@Gel groups exhibited normal morphology and cellular arrangement (Figure 6B). Additionally, the conjunctival epithelial cells were densely arranged and populated with a significant number of goblet cells (Figure 6B). The integrity of the iris and retina was maintained. These results showed the absence of inflammatory changes, inflammatory cell infiltration, or pathological changes in the cornea, conjunctiva, iris, and retina, indicating favorable ocular biocompatibility and tolerance of C-dots and C-dots@Gel.

The biocompatibility of C-dots and C-dots@Gel to mice was evaluated by H&E staining. Compared with the control group, no signs of pathological damage were found in the organs of mice in the administration group, indicating that the C-dots and C-dots@Gel showed no systematic toxicity (Figure 7A). In addition, the blood routine parameters such as red blood cells (RBC), white blood cells (WBC), platelets (PLT), and hemoglobin (GLB) in the three groups were all in the normal range, and they exhibited no significance (Figure 7B–E). All the results indicated that C-dots and C-dots@Gel had better biocompatibility in vivo.

The Therapeutic Efficiency of C-dots@Gel

Benzalkonium chloride (BAC), a prevalent preservative utilized in numerous eye drops, is identified as a significant contributor to the discomforting symptoms associated with DED in clinical practice.[45] To establish an experimental mouse model of DED, 0.2% BAC was applied topically to the ocular surface for 14 consecutive days (Figure 8A and B). The clinical presentation and histopathological alterations induced by BAC in DED closely resemble those observed in human DED, which lead to ocular surface damage, tear film instability, and corneal epithelial lesions, resulting in DED

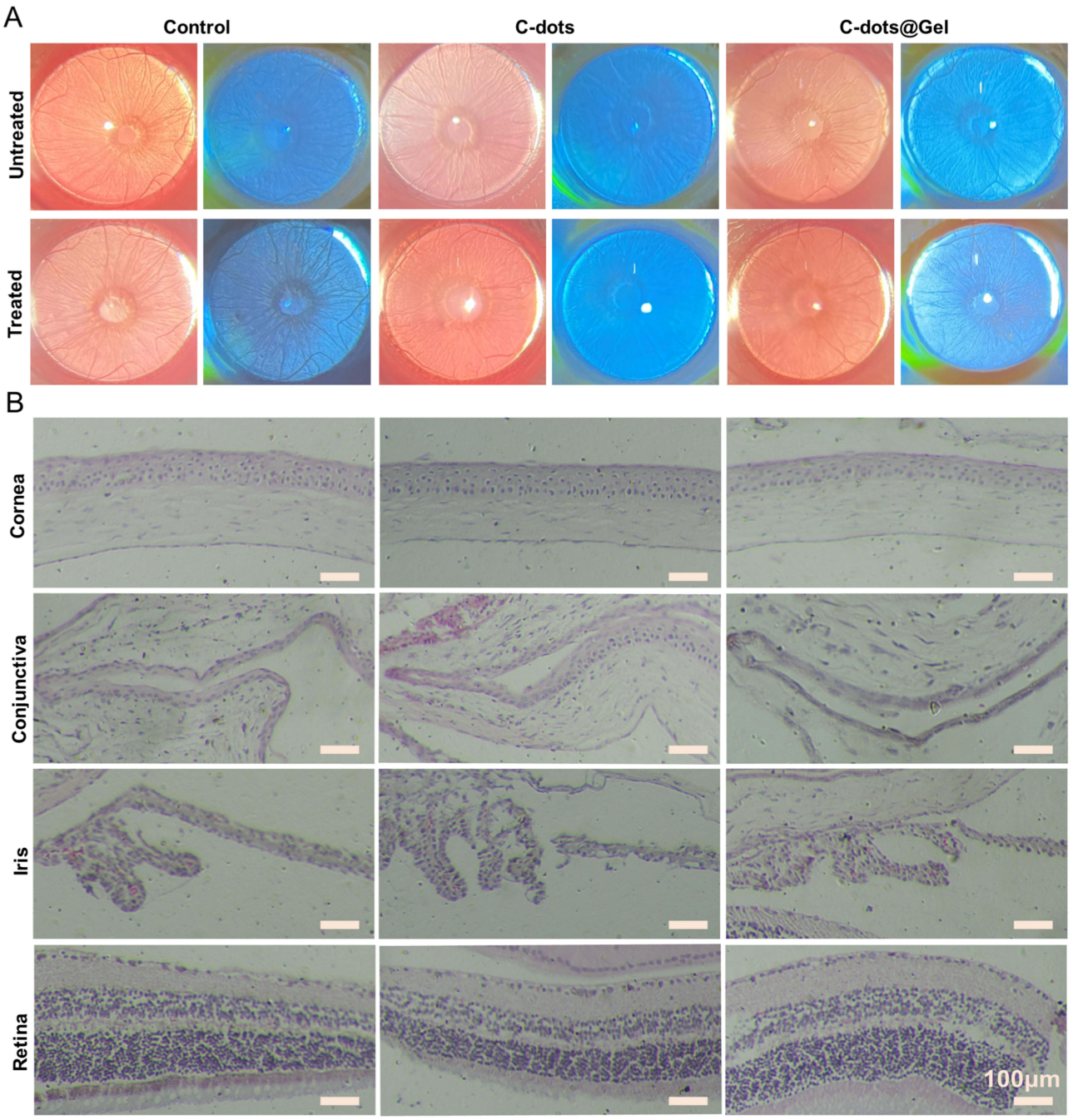

Figure 6 The ocular surface irritation. (**A**) The images of corneal fluorescein sodium staining. (**B**) Histopathology images of ocular tissues (cornea, conjunctiva, iris, retina). Scale bar: 100 μm.

symptoms.[46] The established DED model was assessed primarily through the evaluation of tear volume (SIT), TBUT, and corneal fluorescein staining score (FL).[47] Compared to the control group, the DED group exhibited decreased SIT and TUBT (Figure 8C and D) and increased FL (Figure 8E), indicating the successful preparation of the DED model. There was no statistically significant variance in SIT, TBUT, and FL between the left and right eyes of each mouse ($P > 0.05$), indicating the consistency of the DED model establishment. Moreover, there was no significant differences in the weight changes between the two groups ($P > 0.05$), indicating that BAC did not affect the body weight of mice (Figure 8F).

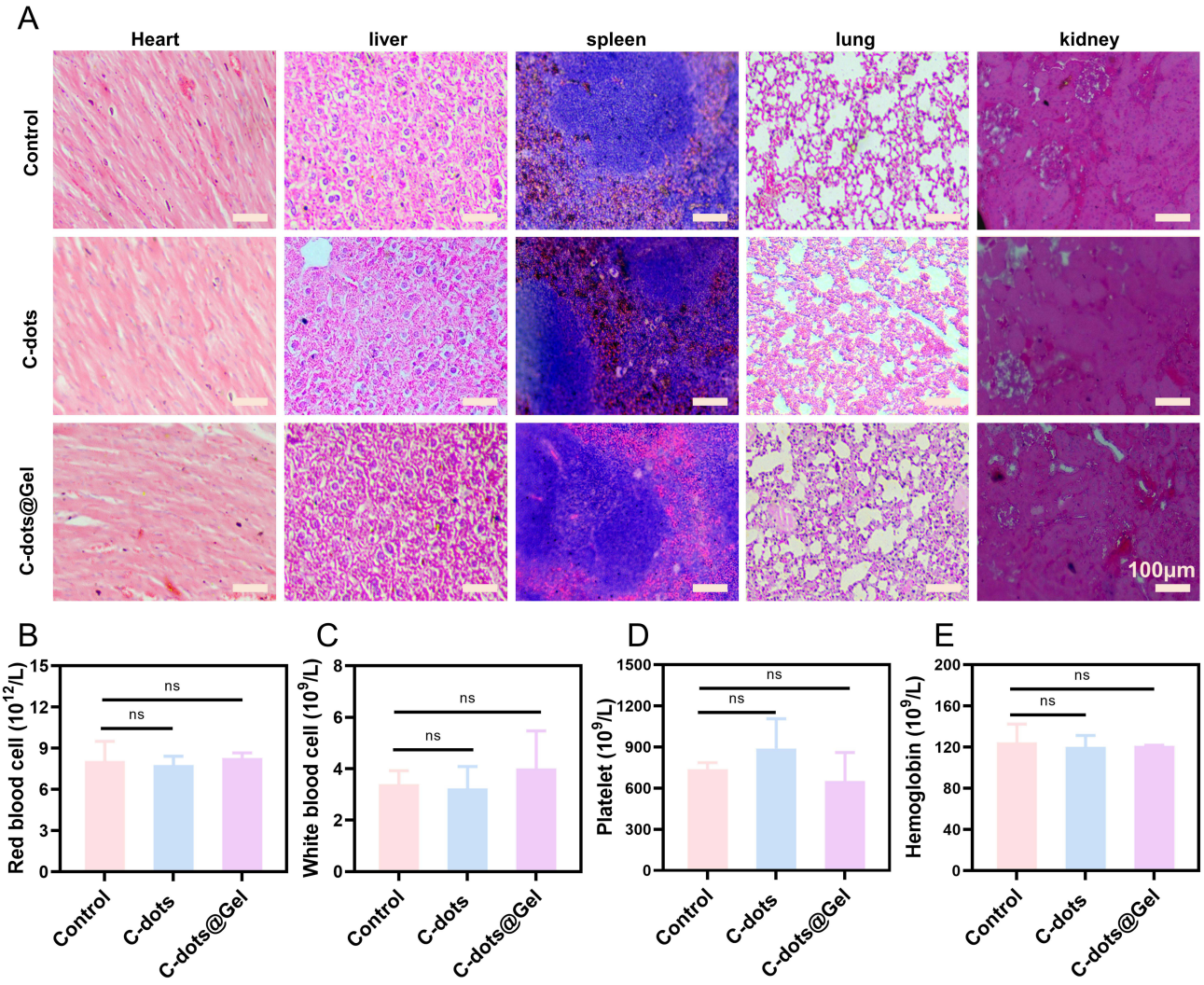

Figure 7 The biocompatibility in vivo. (**A**) Representative histological images of the heart, liver, spleen, lung, and kidney. Scale bar: 100 μm. (**B**–**E**) Main indexes of RBC, WBC, PLT, and HGB blood routine examination. ns, no significance.

The diminished tear volume is a prominent symptom caused by BAC, and is also a key criterion for the clinical diagnosis of DED.[48] Consequently, our investigation focused on the impact of C-dots and C-dots@Gel treatments on tear volume alterations in DED model mice. The tear volume measurements for mice in the DED group, C-dots group, and C-dots@Gel were 2.63±0.11 mm, C-dots, and C-dots@Gel were 4.53±0.49 mm and 4.57±0.56 mm, respectively. Significantly elevated tear volumes were observed in mice treated with C-dots and C-dots@Gel mice compared to those in the DED group ($P < 0.01$) (Figures 8G and 9B–D). These results showed that C-dots and C-dots@Gel exhibited a restorative effect on tear volume reduction in DED mice caused by BAC.

Studies have found that the use of eye drops containing BAC preservatives can result in instability of tear film and a decrease in tear film break-up time,[49] which is a key diagnostic criterion for DED. The impacts of C-dots or C-dots@Gel treatment on tear film rupture time were studied. The tear film break-up time of mice in the DED group, C-dots, and C-dots@Gel were 4.33±0.44 s, 6.0±0.67 s and 6.67±0.44 s, respectively. Both treatment groups showed a longer tear film break-up time compared to the DED group (Figure 8H). However, only a statistical difference ($P < 0.05$) was observed between the DED group and C-dots@Gel (Figure 8H). Longer tear film break-up time means a more stable tear film.[50] The results indicated that C-dots@Gel is conducive to the recovery of tear film in DED mice.

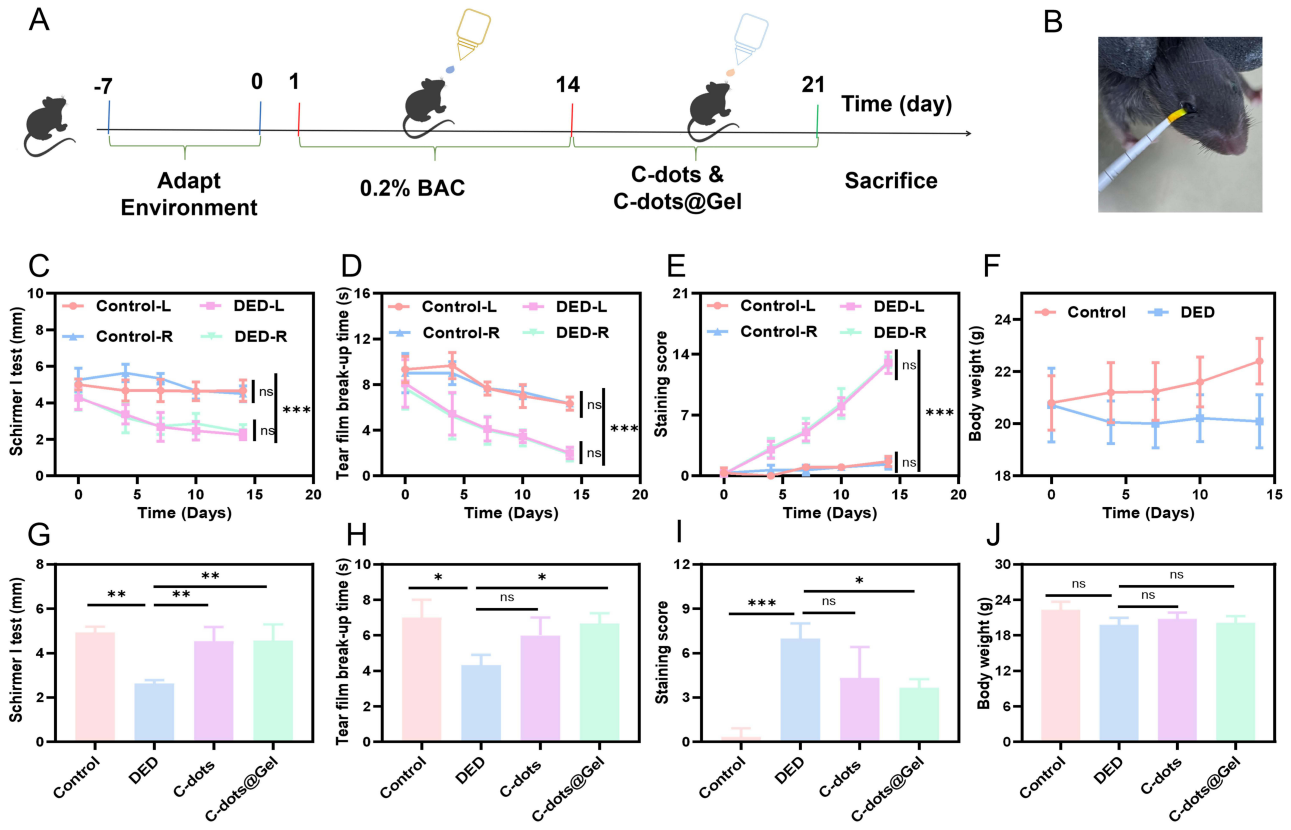

Figure 8 Estabilishment of DED model and In vivo therapeutic effect of Dry eye disease. (**A**) The flow chart of the experiment. (**B**) Tear secretion test diagram. (**C**) Schirmer I test, (**D**) Tear film break-up time, (**E**) Corneal fluorescein staining scores, and (**F**) Body weight during the preparation of the DED model. (**G**) Schirmer I test, (**H**) Tear film break-up time, (**I**) Corneal fluorescein staining scores, and (**J**) Body weight of the DED mice after treatment with C-dots or C-dots@Gel for 7 days (n=3) *, P <0.05; **, P < 0.01; ***, P < 0.001.

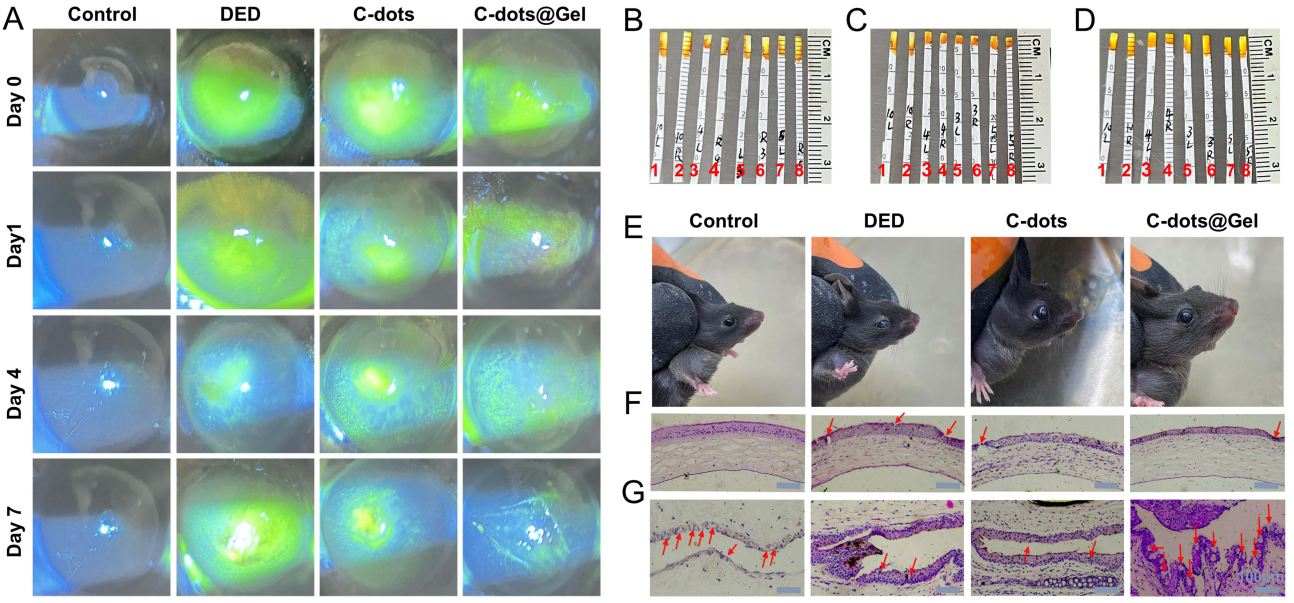

Figure 9 In vivo therapeutic effect of Dry eye disease. (**A**) Images of the fluorescein staining. (**B-D**) Tear filter strip diagram of normal mice (**B**), DED mice (**C**), and DED mice after dropping C-dots or C-dots@Gel on the eye surface (**D**) (Control (1, 2), DED (3, 4), C-dots (5, 6), C-dots@Gel (7, 8). L-Left eye, R-Right eye). (**E**) Appearance of mouse eye surface. (**F** and **G**) Histological images of cornea and conjunctiva from normal mice, DED mice, and DED mice treated with C-dots or C-dots@Gel for 7 days. (**F**) The corneal is indicated by the red arrows. Scale bar: 100 μm. (**G**) Goblet cells in the conjunctiva are indicated by the red arrows. Scale bar: 100 μm.

Corneal fluorescein sodium staining is a valuable tool for assessing corneal epidermal lesions[51] and plays a crucial role in the clinical diagnosis of DED.[52] Studies have demonstrated that BAC can lead to corneal epithelial damage and an increase in corneal epithelial fluorescein staining.[53,54] The extent of corneal fluorescence staining indicated by the green area, which correlates with the severity of epithelial defects.[55] On the 7th day of administration, corneal sodium fluorescein staining of mice in each group was evaluated. The scores of the DED group, C-dots group, and C-dots@Gel group were 7.0±0.67, 4.33±1.56, and 3.67±0.44, respectively. Significantly decreased corneal fluorescence staining scores were observed in C-dots@Gel mice compared to the DED group ($P < 0.05$) (Figure 8I). The results showed that C-dots@Gel was effective in promoting corneal injury repair in DED mice, with C-dots@Gel demonstrating superior efficacy over C-dots. There was no significant difference in the weight of the mice in the C-dots and C-dots@Gel groups when compared with the DED group ($P > 0.05$), indicating that neither C-dots nor C-dots@Gel had an impact on the body weight of mice (Figure 8J).

By analyzing the corneal fluorescence stained areas of mice in each group at various time points (days 0, 1, 4, and 7) it was found that the corneal green fluorescence areas of mice treated with C-dots and C-dots@Gel exhibited varying degrees of reduction over time, indicating a gradual recovery of corneal tissue damage post-administration (Figure 9A).

The control group of mice displayed normal bright eyes with no apparent corneal injury or eyelid edema, while the mice of the DED group exhibited symptoms such as eye rubbing movements, dull eyes, grayish-white corneal surface, and edema of eyelid tissues. The symptoms of mice improved following administration of C-dots and C-dots@Gel, resulting in the disappearance of eyelid tissue edema. Mice in the C-dots@Gel group exhibited bright eyes, while the grayish-white area of the corneal surface decreased in the C-dots group (Figure 9E).

BAC was found to act as a penetrating agent that disrupted corneal barrier function, leading to significant corneal epithelial thinning and damage in mice, which may indicate the progression of DED.[56] The therapeutic efficacy was evaluated through optical microscope pathological analysis of the corneal and conjunctival tissue of mice in each group. In the control group, the corneal tissue exhibited intact cell morphology, characterized by a wide and thick upper cortex neatly arranged Epithelial cells, and tightly arranged stromal layer cells devoid of any discernible pathological features. Conversely, in the DED group, the corneal tissue displayed a thinned upper layer, reduced and disorganized cell layers, the presence of vacuoles, and are as of missing epithelial layer surfaces. Additionally, the stromal layer exhibited a loose arrangement, infiltration of inflammatory cells, and instances of missing cells. After 7 days of C-dots and C-dots@Gel administration, the symptoms were alleviated. Specifically, the upper cortex of the C-dots group exhibited partial thinning with a few vacuoles, whereas the upper cortex of the C-dots@Gel group displayed thickening with orderly arranged stromal layer cells. These findings suggest that both C-dots and C-dots@Gel possess a therapeutic effect on dry corneal injury, with C-dots@Gel demonstrating superiority over C-dots (Figure 9F).

The goblet cells of the conjunctiva play a crucial role in secreting mucous proteins to lubricate and protect the eye surface. Exposure to 0.2% BAC not only led to the infiltration of inflammatory factors in the conjunctiva tissue but also resulted in a decrease in the number of goblet cells in the conjunctiva,[57] causing instability of the tear film and damage to the corneal surface. The reduction in goblet cells is indicative of the progression of DED. In contrast, the control group exhibited a tightly arranged layer of conjunctival epithelial cells with a significant distribution of goblet cells among them. The DED group exhibited a significant increase in epithelial cell layers and a decrease in goblet cells. Following a 7-day treatment with C-dots and C-dots@Gel, both groups experienced an increase in goblet cells. The number of goblet cells in the C-dots@Gel group was higher than that in the C-dots group. C-dots were found to have a restorative effect on the reduction of conjunctival goblet cells in dry eyes, with C-dots@Gel showing superior efficacy over C-dots (Figure 9G).

Conclusion

In this study, a thermosensitive in situ gel system containing C-dots nanozyme was successfully prepared for the treatment of DED. The blank in situ gel was loaded with C-dots nanozyme, which was prepared using P407, P188, and HEMC E50. A 3^2 factorial design approach was employed to optimize the composition and process parameters of the in situ gel. Through visual inspection, it was determined that C-dots@Gel exhibited a light yellow clarified collosol appearance, with uniform dispersion and absence of agglomerates or insoluble impurities. The pH value of the hydrogel

preparation was measured to be approximately 6.5 using a pH meter, which is consistent with the pH range typically found in ophthalmic preparations. When C-dots@Gel is applied to animals, the C-dots@Gel could rapidly form a hydrogel on the mouse eye surface, leading to prolonged retention of the drug on the ocular surface. There was no apparent ocular surface irritation or systemic toxicity observed, indicating favorable biosafety in vivo. A mouse model of DED was established using BAC to assess the therapeutic efficacy of this preparation on DED. The results demonstrated that C-dots@Gel treatment of DED resulted in stabilization of the tear film, prolongation of tear secretion, repair of corneal surface damage, and an increase in the number of conjunctival goblet cells. In comparison to conventional dosage forms, the C-dots nanozyme thermosensitive in situ gel system primarily extended the residence time of C-dots on the ocular surface and enhanced the bioavailability for improved therapeutic outcomes.

Acknowledgments

We thank Feng Wu at the Biomedical Experimental Center of Xi'an Jiaotong University for their assistance with the histological stain.

Funding

This research was funded by the Shaanxi Province Key Research and Development Plan (2022SF-404), the Project of Xi'an Science and Technology Plan (23YXYJ0010), and the National Science Foundation of Shaanxi (2023-JC-QN-081).

Disclosure

The authors declare no conflicts of interest in this work.

References

1. Tsubota K, Yokoi N, Shimazaki J, et al. New perspectives on dry eye definition and diagnosis: a consensus report by the Asia dry eye society. *Ocul Surf*. 2017;15:65–76. doi:10.1016/j.jtos.2016.09.003
2. Craig JP, Nichols KK, Akpek EK, et al. TFOS DEWS II Definition and Classification Report. *Ocul Surf*. 2017;15:276–283. doi:10.1016/j.jtos.2017.05.008
3. Barros A, Lozano-Sanroma J, Queiruga-Piñeiro J, et al. Recovery of corneal innervation after treatment in dry eye disease: a confocal microscopy study. *J Clin Med*. 2023;12:1841. doi:10.3390/jcm12051841
4. Alkhaldi SA, Allam KH, Radwan MA, Sweeney LE, Alshammeri S. Estimates of dry eye disease in Saudi Arabia based on a short questionnaire of prevalence, symptoms, and risk factors: the Twaiq Mountain Eye Study. *Cont Lens Anterior Eye*. 2023;45:763–767. doi:10.1016/j.clae.2022.101770
5. Morthen MK, Magno MS, Utheim TP, Hammond CJ, Vehof J. The work-related burden of dry eye. *Ocul Surf*. 2023;28:30–36. doi:10.1016/j.jtos.2023.01.006
6. Tsubota K, Yokoi N, Watanabe H, et al. A new perspective on dry eye classification: proposal by the Asia dry eye society. *Eye Contact Lens*. 2020;46:S2–S13. doi:10.1097/ICL.0000000000000643
7. Seen S, Tong L. Dry eye disease and oxidative stress. *Acta Ophthalmol*. 2017;96:4. doi:10.1111/aos.13526
8. Chu D, Zhao M, Rong S, et al. Dual-atom nanozyme eye drops attenuate inflammation and break the vicious cycle in dry eye disease. *Nano-Micro Lett*. 2024;16:120. doi:10.1007/s40820-024-01322-7
9. Yu F, Zheng M, Zhang A, Han Z. A cerium oxide loaded glycol chitosan nano-system for the treatment of dry eye disease. *J Control Release*. 2019;315:40–54. doi:10.1016/j.jconrel.2019.10.039
10. Yang D, Han Y, Wang Y, et al. Highly effective corneal permeability of reactive oxygen species-responsive nano-formulation encapsulated cyclosporine a for dry eye management. *Chem Eng J*. 2023;469:143968. doi:10.1016/j.cej.2023.143968
11. Wu Y, Liu Y, Li X, et al. Research progress of in-situ gelling ophthalmic drug delivery system. *Asian J Pharm Sci*. 2019;14:1–15. doi:10.1016/j.ajps.2018.04.008
12. Jumelle C, Gholizadeh S, Annabi N, Dana R. Advances and limitations of drug delivery systems formulated as eye drops. *J Control Release*. 2020;321:1–22. doi:10.1016/j.jconrel.2020.01.057
13. Yang C, Anand A, Huang C, Lai J. Unveiling the power of gabapentin-loaded nanoceria with multiple therapeutic capabilities for the treatment of dry eye disease. *ACS Nano*. 2023;17:25118–25135. doi:10.1021/acsnano.3c07817
14. Jian H, Anand A, Lai J, et al. In situ hybridization of polymeric curcumin to arginine-derived carbon quantum dots for synergistic treatment of bacterial infections. *ACS Appl. Mater. Interfaces*. 2023;15:26457–26471. doi:10.1021/acsami.3c04316
15. Yang C, Nguyen D, Lai J. Poly(l-Histidine)-mediated on-demand therapeutic delivery of roughened ceria nanocages for treatment of chemical eye injury. *Adv Sci*. 2023;10:2302174. doi:10.1002/advs.202302174
16. Ger T, Yang C, Ghosh S, Lai J. Biofunctionalization of nanoceria with sperminated hyaluronan enhances drug delivery performance for corneal alkali burn therapy. *Chem Eng J*. 2023;476:146864. doi:10.1016/j.cej.2023.146864
17. Luo L, Lai J. Epigallocatechin gallate-loaded gelatin-g-Poly(N-Isopropylacrylamide) as a new ophthalmic pharmaceutical formulation for topical use in the treatment of dry eye syndrome. *Sci Rep*. 2017;7:9380. doi:10.1038/s41598-017-09913-8
18. Luo L, Nguyen D, Lai J. Long-acting mucoadhesive thermogels for improving topical treatments of dry eye disease. *Mater Sci Eng C*. 2020;115:111095. doi:10.1016/j.msec.2020.111095

19. Pan M, Ren Z, Ma X, et al. A biomimetic peptide–drug supramolecular hydrogel as eyedrops enables controlled release of ophthalmic drugs. *Acta Biomater*. 2023;167:195–204. doi:10.1016/j.actbio.2023.06.036
20. Liu H, Bi X, Wu Y, et al. Cationic self-assembled peptide-based molecular hydrogels for extended ocular drug delivery. *Acta Biomater*. 2021;131:162–171. doi:10.1016/j.actbio.2021.06.027
21. Yu X, Zhang Z, Yu J, Chen H, Li X. Self-assembly of a ibuprofen-peptide conjugate to suppress ocular inflammation. *Nanomed Nanotechnol Biol Med*. 2018;14:185–193. doi:10.1016/j.nano.2017.09.010
22. Khan N, Aqil M, Ameeduzzafar Imam S, Ali A. Development and evaluation of a novel in situ gel of sparfloxacin for sustained ocular drug delivery: in vitro and ex vivo characterization. *Pharm Dev Technol*. 2015;20:662–669. doi:10.3109/10837450.2014.910807
23. Li J, Zhao H, Okeke C, et al. Comparison of systemic absorption between ofloxacin ophthalmic in situ gels and ofloxacin conventional ophthalmic solutions administration to rabbit eyes by HPLC–MS/MS. *Int J Pharm*. 2013;450(1–2):104–113. doi:10.1016/j.ijpharm.2013.04.018
24. Deshmukh R, Singh R, Mishra S. Pharmaceutical in situ gel for glaucoma: recent trends and development with an update on research and patents. *Crit Rev Ther Drug Carrier Syst*. 2024;41:1–44.
25. Gao W, He J, Chen L, et al. Deciphering the catalytic mechanism of superoxide dismutase activity of carbon dot nanozyme. *Nat Commun*. 2023;14:160. doi:10.1038/s41467-023-35828-2
26. Sharma S, Umar A, Sood S, Mehta SK, Kansal SK. Photoluminescent C-dots: an overview on the recent development in the synthesis, physiochemical properties and potential applications. *J Alloys Compd*. 2018;748:818–853. doi:10.1016/j.jallcom.2018.03.001
27. Wang L, Pan H, Gu D, et al. A novel carbon dots/thermo-sensitive in situ gel for a composite ocular drug delivery system: characterization, ex-vivo imaging, and in vivo evaluation. *Int J Mol Sci*. 2021;22:9934. doi:10.3390/ijms22189934
28. Jian H, Wu R, Lin T, et al. Super-cationic carbon quantum dots synthesized from spermidine as an eye drop formulation for topical treatment of bacterial keratitis. *ACS Nano*. 2017;11:6703–6716. doi:10.1021/acsnano.7b01023
29. Lin H, Wang S, Mao J, et al. Carbonized nanogels for simultaneous antibacterial and antioxidant treatment of bacterial keratitis. *Chem Eng J*. 2021;411:128469. doi:10.1016/j.cej.2021.128469
30. Anand A, Jian H, Huang H, et al. Anti-angiogenic carbon nanovesicles loaded with bevacizumab for the treatment of age-related macular degeneration. *Carbon*. 2023;201:362–370. doi:10.1016/j.carbon.2022.09.045
31. Jian H, Anand A, Lai J, et al. Ultrahigh-efficacy VEGF neutralization using carbonized nanodonuts: implications for intraocular anti-angiogenic therapy. *Adv Healthcare Mater*. 2023;13:2302881. doi:10.1002/adhm.202302881
32. Patel N, Nakrani H, Raval M, Sheth N. Development of loteprednol etabonate-loaded cationic nanoemulsified in-situ ophthalmic gel for sustained delivery and enhanced ocular bioavailability. *Drug Deliv*. 2016;23:3712–3723. doi:10.1080/10717544.2016.1223225
33. Lin P, Jian H, Li Y, et al. Alleviation of dry eye syndrome with one dose of antioxidant, anti-inflammatory, and mucoadhesive lysine-carbonized nanogels. *Acta Biomater*. 2022;141:140–150. doi:10.1016/j.actbio.2022.01.044
34. Niyompanich J, Chuysinuan P, Pavasant P, Supaphol P. Development of thermoresponsive poloxamer in situ gel loaded with gentamicin sulfate for cavity wounds. *J Polym Res*. 2021;28:128. doi:10.1007/s10965-020-02352-6
35. Wei G, Xu H, Ding PT, Li SM, Zheng JM. Thermosetting gels with modulated gelation temperature for ophthalmic use: the rheological and gamma scintigraphic studies. *J Control Release*. 2002;83:65–74. doi:10.1016/s0168-3659(02)00175-x
36. Paradkar MU, Parmar M. Formulation development and evaluation of Natamycin niosomal in-situ gel for ophthalmic drug delivery. *J Drug Deliv Sci Technol*. 2017;39:113–122. doi:10.1016/j.jddst.2017.03.005
37. Hu Y, Wang Y, Deng J, et al. Enzyme-instructed self-assembly of peptide-drug conjugates in tear fluids for ocular drug delivery. *J Control Release*. 2022;344:261–271. doi:10.1016/j.jconrel.2022.03.011
38. Kang SW, Kim K-A, Lee CH, et al. A standardized extract of Rhynchosia volubilis Lour. exerts a protective effect on benzalkonium chloride-induced mouse dry eye model. *J Ethnopharmacol*. 2018;215:91–100. doi:10.1016/j.jep.2017.12.041
39. Yang YT, Wei BJ, Zhao Y, et al. Effects of electroacupuncture on conjunctival cell apoptosis and the expressions of apoptosis-related proteins Caspase-3, Fas and Bcl-2 in rabbits with dry eye syndrome. *J Acupunct Tuina Sci*. 2020;18:16–23. doi:10.1007/s11726-020-1152-5
40. Sung MS, Li Z, Cui L, et al. Effect of Topical 5-Aminoimidazole-4-carboxamide-1-β-d-ribofuranoside in a mouse model of experimental dry eye. *Invest Opthalmol Vis Sci*. 2015;56:3149–3158. doi:10.1167/iovs.14-16153
41. Wang L, Pan H, Gu D, Li P, Su Y, Pan W. A composite system combining self-targeted carbon dots and thermosensitive hydrogels for challenging ocular drug delivery. *J Pharm Sci*. 2022;111:1391–1400. doi:10.1016/j.xphs.2021.09.026
42. HØRven I. Corneal temperature in normal subjects and arterial occlusive disease. *Acta Ophthalmol*. 2009;53:863–874. doi:10.1111/j.1755-3768.1975.tb00404.x
43. Girardin F, Collum M, Erb C, Flammer J. Relationship between corneal temperature and finger temperature. *Arch Ophthalmol*. 1999;117:166–169. doi:10.1001/archopht.117.2.166
44. Barse R, Kokare C, Tagalpallewar A. Influence of hydroxypropyl methylcellulose and poloxamer composite on developed ophthalmic in situ gel: ex vivo and in vivo characterization. *J Drug Deliv Sci Technol*. 2016;33:66–74. doi:10.1016/j.jddst.2016.03.011
45. Jin K, Ge Y, Ye Z, et al. Anti-oxidative and mucin-compensating dual-functional nano eye drops for synergistic treatment of dry eye disease. *Appl Mater Today*. 2022:27. doi:10.1016/j.apmt.2022.101411
46. Carpena-Torres C, Pintor J, Pérez de Lara MJ, et al. Optimization of a rabbit dry eye model induced by topical instillation of benzalkonium chloride. *J Ophthalmol*. 2020;2020:1–10. doi:10.1155/2020/7204951
47. Yi HC, Lee YP, Shin YJ. Influence of nasal tear osmolarity on ocular symptoms related to dry eye disease. *Am J Ophthalmol*. 2018;189:71–76. doi:10.1016/j.ajo.2018.02.008
48. Goto E, Dogru M, Fukagawa K, et al. Successful tear lipid layer treatment for refractory dry eye in office workers by low-dose lipid application on the full-length eyelid margin. *Am J Ophthalmol*. 2006;142:264–270. doi:10.1016/j.ajo.2006.03.022
49. Georgiev GA, Yokoi N, Koev K, et al. Surface chemistry study of the interactions of benzalkonium chloride with films of meibum, corneal cells lipids, and whole tears. *Invest Opthalmol Vis Sci*. 2011;52:4645–4654. doi:10.1167/iovs.10-6271
50. O'Brien PD; FRCSI, Collum L. Dry eye: diagnosis and current treatment strategies. *Curr Allergy Asthma Rep*. 2004;4:314–319. doi:10.1007/s11882-004-0077-2
51. Bron AJ, Tiffany JM, Gouveia SM, Yokoi N, Voon LW. Functional aspects of the tear film lipid layer. *Exp Eye Res*. 2004;78:347–360. doi:10.1016/j.exer.2003.09.019

52. Ma B, Pang L, Huang P, et al. Topical delivery of levocarnitine to the cornea and anterior eye by thermosensitive in-situ gel for dry eye disease. *Drug Des Devel Ther*. 2021;15:2357–2373. doi:10.2147/dddt.s309648
53. Qu M, Qi X, Wang Q, et al. Therapeutic effects of STAT3 inhibition on experimental murine dry eye. *Invest Opthalmol Vis Sci*. 2019;60:3776–3785. doi:10.1167/iovs.19-26928
54. Yang Q, Zhang Y, Liu X, Wang N, Song Z, Wu K. A comparison of the effects of benzalkonium chloride on ocular surfaces between C57BL/6 and BALB/c Mice. *Int J Mol Sci*. 2017;18:509. doi:10.3390/ijms18030509
55. Li S, Lu Z, Huang Y, et al. Anti-oxidative and anti-inflammatory micelles: break the dry eye vicious cycle. *Adv Sci*. 2022;9:e2200435. doi:10.1002/advs.202200435
56. Ouyang W, Wu Y, Lin X, et al. Role of CD4+ T helper cells in the development of BAC-induced dry eye syndrome in mice. *Invest Opthalmol Vis Sci*. 2021;62:25. doi:10.1167/iovs.62.1.25
57. Boulton ME, Li C, Song Y, et al. Research on the Stability of a rabbit dry eye model induced by topical application of the preservative benzalkonium chloride. *PLoS One*. 2012;7:e33688. doi:10.1371/journal.pone.0033688